Real-space imaging of macroscopic diffusion and slow flow by singlet tagging MRI

Giuseppe Pileio*[,a], Jean-Nicolas Dumez[a,b], Ionut-Alexandru Pop[a], Joseph T. Hill-Cousins,[a] and Richard C. D. Brown[a]

[a]*School of Chemistry, University of Southampton, SO17 1BJ, Southampton, U.K.*

[b]*Institut de Chimie des Substances Naturelles, CNRS UPR 2301, Avenue de la Terrasse, 91190 Gif-sur-Yvette, France*

Abstract

Magnetic resonance imaging can be used to study motional processes such as flow and diffusion, but the accessible timescales are limited by longitudinal relaxation. The spatially selective conversion from magnetization to long-lived singlet order in designer molecules makes it possible to tag a region of interest for an extended period of time, of the order of several minutes. Here we exploit this concept of "singlet tagging" to monitor diffusion over a macroscopic scale as well as very slow flow.

Keywords

Long-lived states; Flow; Diffusion; Tagging; Magnetic Resonance Imaging;

Highlights

- Diffusion can be monitored in real space and over a macroscopic scale with singlet tagging
- Singlet tagging makes it possible to measure slower flow compared to magnetization tagging with identical hardware
- Designer molecules can be used for ^{1}H and ^{13}C based singlet tagging

*corresponding author: g.pileio@soton.ac.uk

Graphical abstract

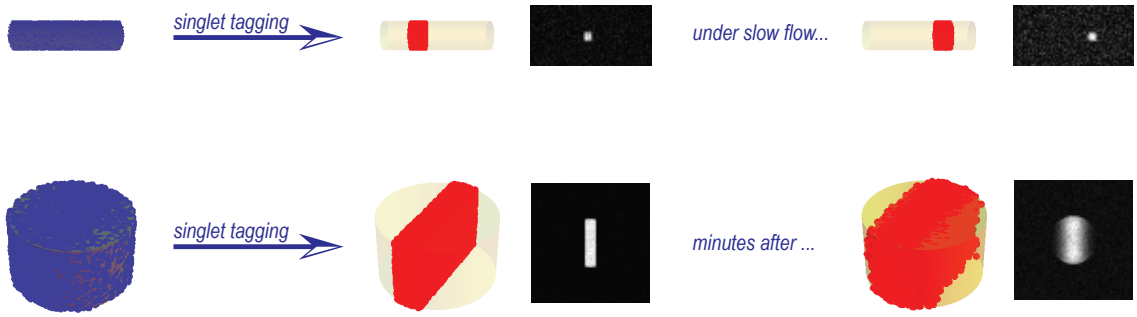

1. Introduction

Beyond anatomical images, magnetic resonance can provide detailed information on motional processes, over a large range of temporal and spatial scales[1–3]. Many techniques rely on the concept of "time-of-flight" imaging, which consists of tagging a region of interest and tracking its subsequent evolution. Alternatively, various forms of motion can be characterized, sometimes quantitatively, with reciprocal-space (q-space) imaging techniques[3], which are applicable on spatial scales smaller than the accessible imaging resolution. The time scales that can be probed with magnetic resonance are, however, constrained by the longitudinal relaxation time, T_1. A region tagged through its magnetization will become indistinguishable from the rest of the sample within several periods of T_1. The study of slow processes thus requires general strategies to extend NMR timescales.

Long-lived states[4] allow spin magnetization to be stored for a considerably extended period of time, typically at least an order of magnitude longer than T_1 for the same molecule. Long-lived states act as repositories of polarization (and hyperpolarisation) that survive the presence of high magnetic fields and are insensitive to radiofrequency fields and field gradient pulses, unless these are played in a very selective manner[5]. This ability to selectively manipulate long-lived states offers the potential for a *smart probe* that can be activated on demand. To date, several strategies have been proposed to manipulate long-lived states[6–10], including highly selective approaches that can be applied in high field and therefore retain all the advantages of a smart probe[8,11]. Recently, we have demonstrated the possibility to convert magnetization to and from singlet order - the prototypical long-lived state formed by a spin pair - in a spatially selective manner, in the high field of a NMR/MRI magnet[12]. These techniques are the basis of "singlet tagging", which consists of converting a portion of a sample into long-lived singlet order, to be revealed at a later time or at a different position in space. Singlet tagging is analogous to spin labeling[13,14], with the advantage that the probe can be followed for a much longer time.

In this communication, we exploit the concept of singlet tagging to access extended timescales in MRI and monitor slow motional processes. For these experiments we make use of two recently synthesized molecules, capable of supporting singlet states with lifetimes of a few minutes. We first study an example of very slow

flow and, subsequently, show how diffusion can be monitored in real space and over a macroscopic distance, once molecules can be tracked for several minutes.

2. Methods

Imaging experiments. All experiments were run on a Bruker 11.7 T Avance III NMR instrument. Two custom molecules (Scheme 1) were used for demonstration purposes.

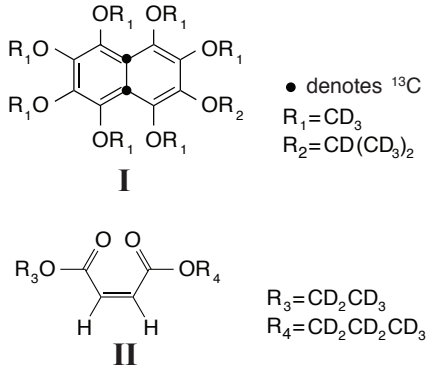

Scheme 1. Molecular schemes of **I**) 1,2,3,4,5,6,8-heptakis(methoxy-d_3)-7-((propan-2-yl-d_7)oxy)-4a,8a-$^{13}C_2$-naphthalene and **II**) 1-(Ethyl-d_5) 4-(propyl-d_7)(*Z*)-but-2-enedioate

Flow imaging experiments were carried out on a 0.8M sample of 1,2,3,4,5,6,8-heptakis(methoxy-d_3)-7-((propan-2-yl-d_7)oxy)-4a,8a-$^{13}C_2$-naphthalene[15] (Scheme 1, **I**) dissolved in $(CD_3)_2CO$. The longitudinal relaxation decay constant of this sample was measured with a standard saturation-recovery experiment and is T_1 = 9 ± 0.1 s. The singlet order decay constant for the same sample was measured as described in Ref. [11] and is T_S = 260 ± 16 s, at 11.7 T and in an undegassed solution (estimated $[O_2]$~2mM at 293.15 K and PO_2=19 kPa). To achieve stationary flow the setup shown in Fig. 1 was used. It consists of a glass chamber (20 mm long, 5 mm OD, 4.2 mm ID) connected through a PTFE hose (0.3 mm ID) to a 2ml injection syringe and a 2 ml recovery syringe (Fig. 1). The injection syringe is mounted on a syringe pump (KD Scientific Inc., USA), which can provide flow rates of up to 120 µl/min for the chosen syringe. The glass chamber sits in the MRI probe. The chamber volume is 280 µl while the *dead* volume of the connection hose is 200 µl. Prior to flow experiments the injection syringe, the glass chamber and the connection hose were filled with a solution of **I**.

Diffusion imaging experiments were carried out on a 1M sample of 1-(ethyl-d5),4-(propyl-d7)(*Z*)-but-2-enedioate[12] (Scheme 1, **II**) dissolved in CD_3CN. The sample was degassed by 4 pump-thaw cycles (to remove paramagnetic oxygen and

therefore increase T_1 and T_S) and sealed into a 5 mm OD J-Young valve NMR tube. The longitudinal relaxation decay constant of this sample is T_1 = 19.6 ± 0.2 s; its singlet order decay constant is T_S = 360 ± 30 s.

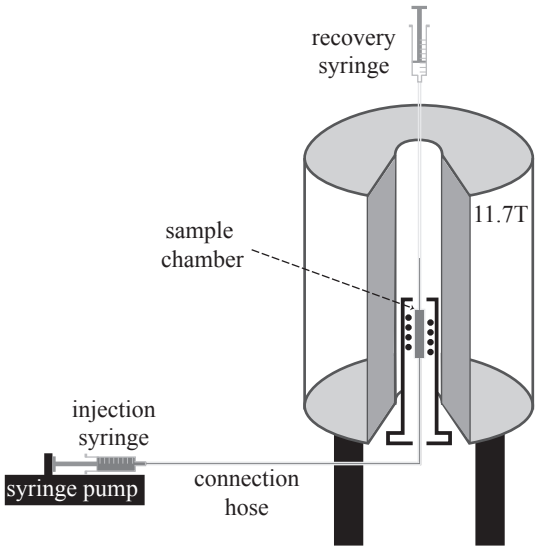

Figure 1. Equipment used for imaging of slow flow.

All MRI experiments were performed on a micro-imaging probe coupled to a gradient system delivering up to 150 G/cm, using a 10 mm ^{1}H coil for diffusion measurements and a 10 mm ^{1}H/^{13}C coil for flow measurements. 2D images were obtained with a RARE MRI pulse sequence[16]. Vendor-provided sinc-3 pulses with duration of 1 ms were used to select sagittal and axial slices in the sM2S (Fig. 2b) for the macroscopic diffusion and slow flow experiments, respectively. Custom Paravision (Bruker, Billerica, MA) pulse sequences were used and the experimental data were processed with custom Mathematica (Wolfram Research Inc., Champaign, IL) routines.

Simulation of diffusion. Numerical simulations of diffusion were performed with Mathematica. A configuration of 100,000 molecules, initially confined in a sagittal slice of 0.9 mm thickness and 20 mm height was allowed to undergo random walk diffusion to reach a final configuration after a diffusion time of 10 μs, 1, 2, 3 and 5 minutes, in separate runs. Diffusion was confined within a cylinder of 4.2 mm diameter and 20 mm height that mimic the sample used in the diffusion experiments below. Pseudo-images were obtained as 2D arrays by counting the number of molecules in each voxel, with voxel geometry chosen to match the experimental one. Simulated images include randomly generated noise to match the experimental signal-to-noise ratio and an exponential decay of intensity, with a decay rate constant of 360 s, to account for singlet relaxation.

3. Results and Discussion

Singlet tagging. Singlet tagging refers to the spatially selective conversion from magnetization to long-lived singlet order (sM2S) in a solution of singlet-bearing molecules[12]. The pulse sequence used for singlet tagging experiments is shown in Fig. 2a. During the sM2S block, longitudinal magnetization is converted into singlet order only in a selected slice of the sample - the geometry of the selected slice is chosen through the parameters of the selective pulses and field gradients. After creation of singlet order, a variable time interval *t* is left, during which the tagged molecules may move. Because of the long lifetime of singlet states in suitable molecules such as **I** (T_s~260 s) and **II** (T_s~360 s), *t* can be up to several minutes and still yield images with suitable signal-to-noise ratio. After the delay *t*, a singlet filter[17] is used to destroy magnetization or any term other than singlet order (up to rank 3) that may have been created during *t*. A non-selective singlet-to-magnetization sequence (Fig. 2c) is run to reconvert singlet order into longitudinal magnetization. At this point, the spatial configuration of the tagged molecules can be interrogated by any suitable imaging technique. Here we have used a single-shot version of the RARE[16] pulse sequence, which provides both high sensitivity and a high robustness against field inhomogeneity. Although RARE is not typically used as a single-shot technique, the long transverse relaxation times of the two compounds studied here are compatible with very long echo times.

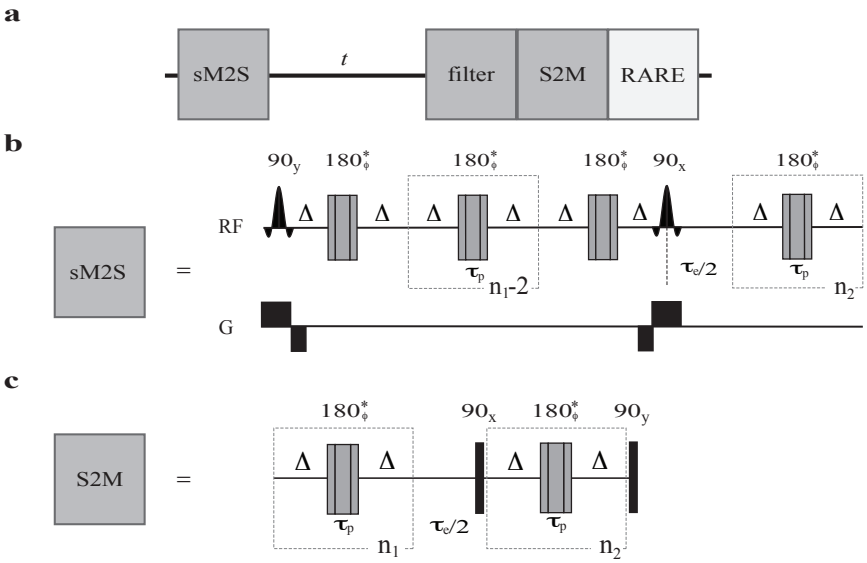

Figure 2. a) Pulse sequence used for singlet tagging experiments; b) details of the sM2S block; c) details of the S2M block. Asterisks indicate a composite 180° pulse built as $90_x180_y90_x$. The

phase ϕ is cycled as [x,x,-x,-x,x,x,-x,-x,-x,-x,x,x,-x,-x,x,x] within the trains of 180° pulses. The total echo time is given as $\tau_e = \tau_p + 2\Delta = 1/(2\sqrt{J^2 + (\Delta\nu)^2})$ with τ_p the duration of the composite 180° pulse. $n_1 = \pi J/(2\Delta\nu)$ and $n_2 = n_1/2$. For the experiments below $n_1 = 12$ and 16, $\Delta =$ 4.55 and 20.8 ms, $\tau_p = 86$ and 64 μs, for compound **I** and **II**, respectively; the duration of the sM2S/S2M blocks are therefore 171.9/169.9 ms for **I** and 1022.7/1020.8 ms for **II**; the filter duration is ~19.9 ms and the duration of the RARE sequence is 607 ms for **I** and 567.5 ms for **II**.

Slow Flow Imaging. The singlet tagging approach can be used to study slow flow with time-of-flight imaging techniques. A stationary flow was obtained here with the equipment shown in Fig. 1 where the flow speed is controlled by a syringe pump. The experiment started by filling the injection syringe, the glass chamber and the connection hose with a 0.8M solution of **I** dissolved in $(CD_3)_2CO$. A 2D single-shot RARE image of a 10 mm thick sagittal slice of the sample is shown in Fig. 3a, in the absence of flow, to reveal the geometry of the sample.

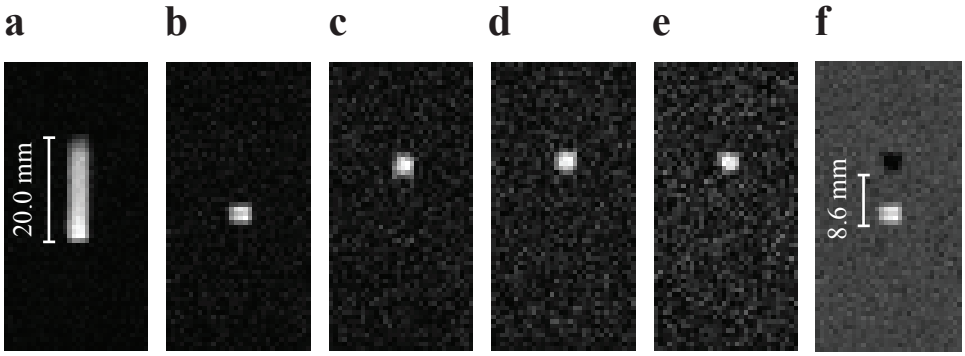

Figure 3. Measurement of slow flow with singlet tagging in a 4.2 mm ID x 20 mm H glass chamber containing a 0.8M solution of **I** in $(CD_3)_2CO$. a) singlet-shot RARE image in the absence of flow. (b-e) Images obtained with the pulse sequence in Fig. 2, with the sM2S selective pulse that selects an axial slice of 3.9 mm placed 3 mm away from the bottom edge of the glass. The delays were t = 10μs (b), 1 minute (c), 2 minutes (d) and 3 minutes (e) and under stationary flow of 0 μl/min, 120 μl/min, 60 μl/min and 40 μl/min, from (b) to (e) respectively. f) Difference between image (b) and (e) showing a displacement of 8.6 mm achieved in 3 minutes and corresponding to a net speed of about 50μm/s. All images have FOV = 50 × 25 mm^2, matrix size = 64 × 32, sagittal slice thickness = 10 mm, TE = 18.3 ms, acceleration factor 64.

The pulse sequence in Fig. 2 was then used to monitor the flow, with the sM2S block set to tag as singlet order only molecules present in an axial slice of 3.9 mm thickness, offset from the bottom edge of the sample by about 3 mm. Fig. 3b shows a reference image, obtained under static conditions. Flow experiments were performed with three different delays t: 1, 2 and 3 min, with the resulting images shown in Fig. 3c, 3d and 3e, respectively. The difference between images in Fig. 3b and Fig. 3e, reported in Fig. 3f, highlights the displacement of the region of interest. In each case, the syringe pump was set with a flow rate such that the region of interest would always move by the same

amount (120, 60 and 40 µl/min for the 1, 2 and 3 min experiments, respectively). The pump was started 15 s before the NMR experiment, in order to reach stationary flow conditions. In all three experiments the tagged molecules have moved up in the glass chamber by 8.6 mm. Their velocity is slower by a factor of 2 in Fig. 3d compared to Fig. 3c, and a factor of 3 in Fig. 3e. The flow speed is readily calculated as 142, 71 and 48 µm/s for cases in Fig. 3c, 3d and 3e, respectively. For comparison, flow speeds in the human body can be of the order of 500 µm/s and below, e.g., in blood capillaries and ischemic tissues. Slow flow measurements are also relevant in porous media where flow rates depend on many parameters and can be as slow as 10-100 µm/s for water in sandstone and layered clay or slower than that in limestone and other impervious materials. In porous materials the insensitivity of singlet states to susceptibility gradients may result as an advantage over, for example, phase-contrast methods.

Macroscopic Diffusion Imaging. Diffusion is usually studied in NMR with "reciprocal space" approaches, in which the signal attenuation of a gradient or spin echo is measured as a function of gradient amplitude[2,18–20]. Measurements of slow diffusion coefficients by singlet state spectroscopy have already been reported[21] where singlet state preparation is combined with pulsed field gradients to investigate diffusion constants in reciprocal space. The long lifetime of singlet spin states has also been used to demonstrate the enhancement in q-space imaging of macroscopic pores[22].

The unusually long timescales accessible with singlet tagging make it possible to study diffusion in real rather than reciprocal space. This is illustrated in Fig. 4, where the diffusion of **II** in CD_3CN is monitored. A reference single-shot RARE 2D axial image of the sample is shown in Fig. 4a0. The sM2S sequence was set to tag as singlet order only the molecules located in a 0.9 mm thick sagittal slice at the center of the NMR tube. A series of images were acquired using the pulse sequence in Fig. 2 where the diffusion interval t is varied as 10 µs, 1, 2, 3 and 5 minutes (Fig. 4a1-a5) in each successive run. For t = 10 µs, macroscopic diffusion can be ignored and the geometry of the tagged region can be appreciated (Fig. 4a1). As the time interval t increases, diffusion takes place and, as expected, the singlet-tagged region becomes broader and reduces in intensity (Fig. 4a2-a5). For t = 5 minutes (Fig. 4a5) the singlet-tagged molecules have diffused a macroscopic distance of a few millimeters to occupy all the available volume.

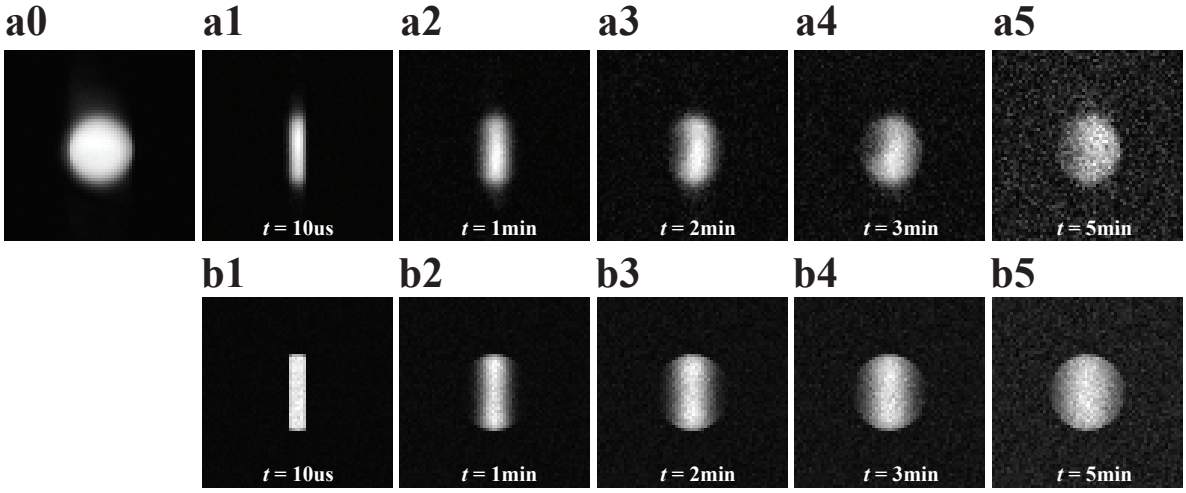

Figure 4. a0) axial RARE image of a 5mm OD (4.2 mm ID) NMR tube containing a degassed 1M solution of **II** in CD_3CN. a1-a5) Real space imaging of macroscopic diffusion obtained by pulse sequence in Fig. 2. The value of the diffusion interval t is indicated. FOV = 20 × 20 mm^2, matrix size = 64 × 64, sagittal slice thickness = 0.9 mm, axial slice thickness = 15 mm, TE = 8.7 ms, acceleration factor 64. b1-b5) Simulation of diffusion in a 5mm OD NMR tube using a random walk model, a diffusion constant of 1.6 10^{-9} m^2 s^{-1} and all other parameters as used in the experiment.

A simple description of Brownian diffusion can be obtained using a mathematical model in which molecules undergo a large number of random movements in real space (random-walk model). In this model, the mean square displacement of a molecule is directly proportional to its diffusion coefficient D and the diffusion time interval t according to $\langle r^2 \rangle = 6Dt$.[23] The diffusion time constant of **II** (1M in CD_3CN at 293.15 K) has been measured using a convection compensated DOSY sequence[24] and is $D_{\mathbf{II}}$ = 1.6×10^{-9} m^2 s^{-1}. This value is inserted in a simulation algorithm written in Mathematica (see Methods). Simulated 2D images, shown in Fig. 4b1-b5, are in good agreement with the experimental images reported in Fig. 4a1-a5.

Thermal convection may also contribute to motion and is a common issue in diffusion NMR techniques. Convection effects due to thermal differences across the sample may be partially responsible for the observed total displacement of the singlet tag in Fig. 4. They were reduced by using a small diameter NMR tube (5mm OD) held inside an empty 10mm OD tube. The good agreement between experiment and simulation confirms the minimal contribution of thermal convection here.

In the two examples shown here, a high concentration of the imaged molecule is needed in order to obtain a suitable spatial resolution. This limitation can be overcome by the use of hyperpolarisation techniques such as dissolution-DNP[25], which leads to a gain of up to 5 orders of magnitude in signal intensity, thus allowing the imaging of

slow flow and macroscopic diffusion in much more diluted samples and/or with a higher spatial resolution. The availability of longer-lived singlet states - singlet bearing molecules with singlet decay constants of tens of minutes have been reported[26–28]- will also give access to real-space imaging of diffusion over longer distances and slower flow rates.

4. Conclusions

In summary, we have demonstrated that singlet-tagging techniques can be used to monitor slow displacements directly with magnetic resonance imaging. A first example is the characterization of slow flow, in a custom-made flow chamber, with a flow of 50 μm/s. A second example is the real-space imaging of diffusion, over a macroscopic distance of a few millimeters. Together these examples illustrate the potential of singlet tagging, which can be used to probe macroscopic channels in materials and, provided that biocompatible agents can be found, in vivo MRI applications. The displacement that can be measured with singlet tagging depends on the lifetime of the singlet order for the chosen molecule. The next generation of singlet-bearing molecules should provide access to timescales that are longer by an order of magnitude or more. This will give access to imaging diffusion over larger distances and slower flow.

Acknowledgments

The authors thank Malcolm H. Levitt and Philip W. Kuchel for insightful discussions, Javier Alonso Valdesueiro for technical help and EPSRC (EP/I036141) and ERC (291044 - HYPERSINGLET) for funding. JND acknowledge the EU-COST action TD1103 for travel funds.

References

[1] P.T. Callaghan, Principles of Nuclear Magnetic Resonance Microscopy, Clarendon Press, 1993.

[2] M.A. Bernstein, K.E. King, X.J. Zhou, W. Fong, Handbook of MRI Pulse Sequences, Med. Phys. 32 (2005) 1452. doi:10.1118/1.1904597.

[3] P.T. Callaghan, Translational Dynamics and Magnetic Resonance, Oxford University Press, 2011. doi:10.1093/acprof:oso/9780199556984.001.0001.

[4] M.H. Levitt, Singlet nuclear magnetic resonance., Ann. Rev. Phys. Chem. 63 (2012) 89–105. doi:10.1146/annurev-physchem-032511-143724.

[5] G. Pileio, S. Bowen, C. Laustsen, M.C.D. Tayler, J.T. Hill-Cousins, L.J. Brown, et al., Recycling and imaging of nuclear singlet hyperpolarization, J. Am. Chem. Soc. 135 (2013) 5084–5088. doi:10.1021/ja312333v.

[6] M. Carravetta, O.G. Johannessen, M.H. Levitt, Beyond the T1 limit: singlet nuclear spin states in low magnetic fields., Phys Rev Lett. 92 (2004) 153003. doi:10.1103/PhysRevLett.92.153003.

[7] M. Carravetta, M.H. Levitt, Long-lived nuclear spin states in high-field solution NMR., J Am Chem Soc. 126 (2004) 6228–6229. doi:10.1021/ja0490931.

[8] G. Pileio, M. Carravetta, M.H. Levitt, Storage of nuclear magnetization as long-lived singlet order in low magnetic field., Proc. Natl. Acad. Sci. U.S.A. 107 (2010) 17135–9. doi:10.1073/pnas.1010570107.

[9] S.J. DeVience, R.L. Walsworth, M.S. Rosen, Preparation of Nuclear Spin Singlet States Using Spin-Lock Induced Crossing, Phys. Rev. Lett. 111 (2013) 173002. doi:10.1103/PhysRevLett.111.173002.

[10] T. Theis, Y. Feng, T. Wu, W.S. Warren, Composite and shaped pulses for efficient and robust pumping of disconnected eigenstates in magnetic resonance., J. Chem. Phys. 140 (2014) 014201. doi:10.1063/1.4851337.

[11] M.C.D. Tayler, M.H. Levitt, Singlet nuclear magnetic resonance of nearly-equivalent spins., Phys. Chem. Chem. Phys. 13 (2011) 5556–60. doi:10.1039/c0cp02293d.

[12] J.-N. Dumez, J.T. Hill-Cousins, R.C.D. Brown, G. Pileio, Long-lived localization in magnetic resonance imaging., J. Magn. Reson. 246 (2014) 27–30. doi:10.1016/j.jmr.2014.06.008.

[13] J.A. Detre, J.S. Leigh, D.S. Williams, A.P. Koretsky, Perfusion imaging, Magn. Reson. Med. 23 (1992) 37–45. doi:10.1002/mrm.1910230106.

[14] D.S. Williams, J.A. Detre, J.S. Leigh, A.P. Koretsky, Magnetic resonance imaging of perfusion using spin inversion of arterial water, Proc. Natl. Acad. Sci. . 89 (1992) 212–216. http://www.pnas.org/content/89/1/212.abstract.

[15] G. Stevanato, J.T. Hill-Cousins, P. Håkansson, S.S. Roy, L.J. Brown, R.C.D. Brown, et al., A Nuclear Singlet Lifetime of more than 1 Hour in Room-Temperature Solution, Angewandte Chemie (2015), *accepted for publication*, DOI: 10.1002/anie.201411978.

[16] J. Hennig, A. Nauerth, H. Friedburg, RARE imaging: A fast imaging method for clinical MR, Magn. Reson. Med. 3 (1986) 823–833. doi:10.1002/mrm.1910030602.

[17] M.C.D. Tayler, M.H. Levitt, Accessing long-lived nuclear spin order by isotope-induced symmetry breaking, J. Am. Chem. Soc. 135 (2013) 2120–2123. doi:10.1021/ja312227h.

[18] D. Le Bihan, E. Breton, D. Lallemand, P. Grenier, E. Cabanis, M. Laval-Jeantet, MR imaging of intravoxel incoherent motions: application to diffusion and perfusion in neurologic disorders., Radiology. 161 (1986) 401–407. doi:10.1148/radiology.161.2.3763909.

[19] J. Frahm, A. Haase, D. Matthaei, Rapid NMR imaging of dynamic processes using the FLASII technique, Magn. Reson. Med. 3 (1986) 321–327. doi:10.1002/mrm.1910030217.

[20] C.S. Johnson, Diffusion ordered nuclear magnetic resonance spectroscopy: principles and applications, Prog. Nucl. Magn. Reson. Spectrosc. 34 (1999) 203–256. doi:10.1016/S0079-6565(99)00003-5.

[21] S. Cavadini, J. Dittmer, S. Antonijevic, G. Bodenhausen, Slow diffusion by singlet state NMR spectroscopy., J. Am. Chem. Soc. 127 (2005) 15744–8. doi:10.1021/ja052897b.

[22] N.N. Yadav, A.M. Torres, W.S. Price, NMR q-space imaging of macroscopic pores using singlet spin states., J. Magn. Reson. 204 (2010) 346–8. doi:10.1016/j.jmr.2010.03.010.

[23] D.A. McQuarrie, Statistical Mechanics, University Science Books, 2000.

[24] A. Jerschow, N. Müller, Suppression of Convection Artifacts in Stimulated-Echo Diffusion Experiments. Double-Stimulated-Echo Experiments, J. Magn. Reson. 125 (1997) 372–375. doi:10.1006/jmre.1997.1123.

[25] J.H. Ardenkjaer-Larsen, B.B. Fridlund, A. Gram, G. Hansson, L. Hansson, M.H. Lerche, et al., Increase in signal-to-noise ratio of > 10,000 times in liquid-state NMR., Proc Natl Acad Sci U S A. 100 (2003) 10158–10163. doi:10.1073/pnas.1733835100.

[26] G. Pileio, M. Carravetta, E. Hughes, M.H. Levitt, The long-lived nuclear singlet state of 15N-nitrous oxide in solution., J Am Chem Soc. 130 (2008) 12582–12583. doi:10.1021/ja803601d.

[27] R.K. Ghosh, S.J. Kadlecek, J.H. Ardenkjaer-Larsen, B.M. Pullinger, G. Pileio, M.H. Levitt, et al., Measurements of the persistent singlet state of N2O in blood and other solvents--potential as a magnetic tracer., Magn. Reson. Med. 66 (2011) 1177–80. doi:10.1002/mrm.23119.

[28] G. Pileio, J.T. Hill-Cousins, S. Mitchell, I. Kuprov, L.J. Brown, R.C.D. Brown, et al., Long-lived nuclear singlet order in near-equivalent 13C spin pairs, J. Am. Chem. Soc. 134 (2012) 17494–17497. doi:10.1021/ja3089873.